

---

## Effects of ozone exposure on free radical signals in photosystem I and on chlorophyll fluorescence in green foxtail, *Setaria viridis* Beauv.

---

U. Mazarura\*

University of Zimbabwe, Crop science department, PO BOX Mp 167 Mt Pleasant, Harare, Zimbabwe

U. Mazarura (2012) Effects of ozone exposure on free radical signals in photosystem I and on chlorophyll fluorescence in green foxtail, *Setaria viridis* Beauv. Journal of Agricultural Technology 8(7):2409-2421.

The mechanism of Tropospheric ozone damage to plants is not well understood. A study to try and bridge that gap was carried out. Studies with a C-4 grass, *Setaria viridis* Beauv., green foxtail, treated with sine-wave exposures to O<sub>3</sub> within the modified cavity of an electron paramagnetic resonance (EPR) spectrometer, permitted observation of the effects of exposure on both the free radical signals in photosystems I and II and on chlorophyll fluorescence attributable to photosystem II. Signal I (from P700<sup>+</sup> in PSI) was stimulated by O<sub>3</sub> suggesting an interference with electron flow. During exposure to O<sub>3</sub>, non-photochemical quenching (qN) decreased over time but remained higher than in the control while NPQ remained unchanged over time but also was consistently higher than in the control, suggesting impairment of electron flow. These observations together with the O<sub>3</sub>-induced increases in non-photochemical quenching and the changes in EPR signals are compatible with the suggestion that interference with water-splitting is a major consequence of exposure to O<sub>3</sub>. The level of Signal I in white light was approximately about twice that in far-red light, presumably because of a contribution by PSII light-harvesting to PSI in the bundle-sheath chloroplasts. Measurements of the relative levels of Signal I in white or far-red light may therefore provide a means of assessing the extent of such contributions in other C-4 species.

**Key words:** signal I, photosystem II, *Setaria viridis*; EPR, free radicals; Signal I; C-4,

### Introduction

Ozone affects plants in many ways, including symptomatic injury such as chlorosis or necrosis and sometimes it causes metabolic changes that are not easily discernible (Heath 1988) but resulting in reduced photosynthesis and decline in growth and yield (L. Wang *et al.* 2008; Angeles Calatayud and Eva Barreno 2004; Zheng, 2010). Theoretically toxic free radicals like superoxide anion and hydroxyl are thought to cause plant injury because of the possibilities

---

\* Corresponding author: U. Mazarura; e-mail: [umazarura@agric.uz.ac.zw](mailto:umazarura@agric.uz.ac.zw)

of their formation during reactions of O<sub>3</sub> with cell constituents and their high reactivity and potential for membrane perturbation (Mudd, 1982).

The photosynthetic electron transport system produces the toxic superoxide radical, but it is scavenged by superoxide dismutase (SOD) and other antioxidants such as ascorbic acid, peroxidase, glutathione and  $\alpha$ -tocopherol thereby reducing its potential toxicity (Dizengremel, 2009). As a result, superoxide-induced adverse effects are thought to be a result of reduced scavenging or elevated production.

Until recently, evidence for the involvement of superoxide in O<sub>3</sub> phytotoxicity has been indirect based mainly on observations of the activity of SOD. Elevated SOD activity from exposure to O<sub>3</sub> was reported in bean (*Phaseolus vulgaris*) (Lee and Bennett, 1982) and in spinach (*Spinacia oleracea*) (Decleire *et al.*, 1984). However direct evidence of superoxide formation in grass and radish leaves exposed to 100ppb O<sub>3</sub>, based on electron paramagnetic resonance (EPR) spectroscopic evidence has been put forward (Runeckles and Vaartnou 1997). Further, recent work in molecular biology has elucidated the involvement of SOD in the response of plants to both abiotic and biotic stresses (Ding, 2010; Zhu *et al.*, 2011; Sunkar *et al.*, 2006).

EPR is a unique and direct method for the detection and characterization of free radical spectra. Two free radical signals associated with the photosynthetic apparatus can be detected in intact leaves *in situ* (Victor and Manivalde, 1992). One is stable and persists in darkness (Signal II) and is thought to be attributable to tyrosine residues on the D1 and D2 peptides of photosystem II (Barry and Babcock, 1987). A second distinct Signal (I) appears in white light, and is stimulated by far-red light (>700nm). Signal I is believed to be a result of oxidized chlorophyll P700 in photosystem I and disappears in darkness (Beinert *et al.*, 1962). In 710nm illumination, Signal I shows successful cyclic electron flow in photosystem I.

Chlorophyll fluorescence measurements have been used by several workers studying the effects of O<sub>3</sub> on a range of plant species since the early report by (Schreiber *et al.*, 1978). Since then, ozone has shown to decrease maximum chlorophyll fluorescence quantum yield (Fv/Fm), actual quantum yield (Y) and photochemical quenching (qP), and to increase non-photochemical quenching (NPQ) (Zheng, 2010; Angeles and Eva, 2004; Wang *et al.*, 2008; Calatayud *et al.*, 2004; Bussotti *et al.*, 2011). Since changes in such fluorescence are attributable to changes in photosystem II, the combination of EPR and fluorescence measurements allow the concurrent observation of effects of O<sub>3</sub> on both photosystems.

The objective of this study was, hence, to study the effects of O<sub>3</sub> on photosystem functioning in intact leaf tissue, utilising EPR measurements of

free radical intermediates in Photosystems I and II, and chlorophyll fluorescence transient kinetics. The studies were done on intact, attached leaves of a C-4 grass, green foxtail

## **Materials and methods**

### ***Plant material and growing condition***

Green foxtail (*Setaria viridis* Beauv.) plants were grown from seed in 5cm pots containing about 500 cc standard potting soil (85 loam; 15% peat) in a greenhouse. A slow release fertiliser, 14:14:14 NPK (Osmocote; Sierra Chemical Company), was applied to the standard potting soil at planting at 0.5g/pot. About 50 seeds were sown per pot and these were thinned to 4 plants per pot, 5 days after sowing. The plantings were staggered in order to provide plants of the same age for the experiments. The plants were grown on the greenhouse bench at  $25 \pm 3^{\circ}\text{C}$  and maximum illumination of  $500 \mu\text{mol m}^{-2} \text{s}^{-1}$  (PAR) and exposed to  $\text{O}_3$  at 6 weeks after sowing.

### ***Exposure to $\text{O}_3$***

The exposures were carried out within the quartz dewar insert in the cavity of the EPR spectrometer (Figure 1). Ozone levels approximated sine waves and were controlled by a program written for a 21X Micrologger (Campbell Scientific Inc. Exposure commenced at 10:00h and the peak (120 ppb) occurred at 14:00h. To maintain a moist airflow over the leaf, compressed air from a cylinder of medical grade air was bubbled through distilled water. The flow rate was approximately  $2 \text{ l min}^{-1}$  through the quartz insert. Ozone was generated in the air stream by means of an ultraviolet source (Delzone Z0.300; Del Industries) and was monitored by sampling through a 3mm OD Teflon tube feeding to a Model 1003-AH  $\text{O}_3$  monitor (Dasibi Environmental Corp).

Overall concentrations of  $\text{O}_3$  were adjusted using needle valve/flow meter combinations to produce the desired maximum concentrations (120ppb). The selection of 120ppb maxima for both pollutants was based in part on the 1-hour average concentrations that are defined in the Federal Air Quality Objectives for Canada (82ppb), and the Air Quality Standards for the United States (120ppb).

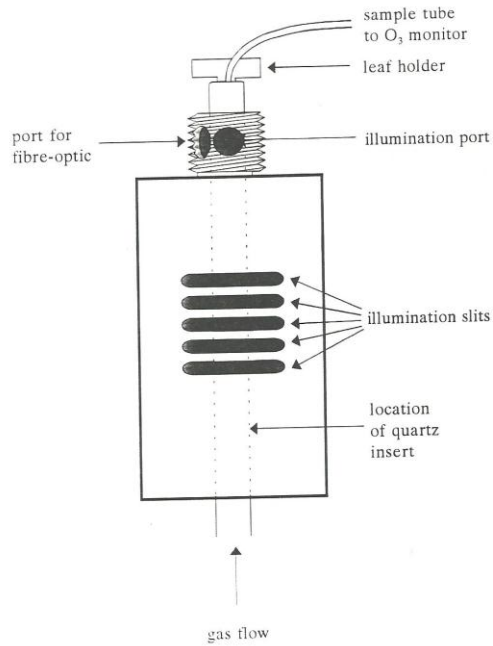


**Fig. 1.** The microwave cavity showing the adaptation of the threaded collar to accommodate the fibre-optic cable of from the fluorometer, and provide an additional illumination port.

Typical exposure regimes for O<sub>3</sub> and the control are given in Figure 2. The curves in Figure 2 were obtained with the distance weighted least squares (DWLS) smoothing function of SYGRAPH (SYSTAT Inc.) and show the typical daytime rise in ambient O<sub>3</sub>.

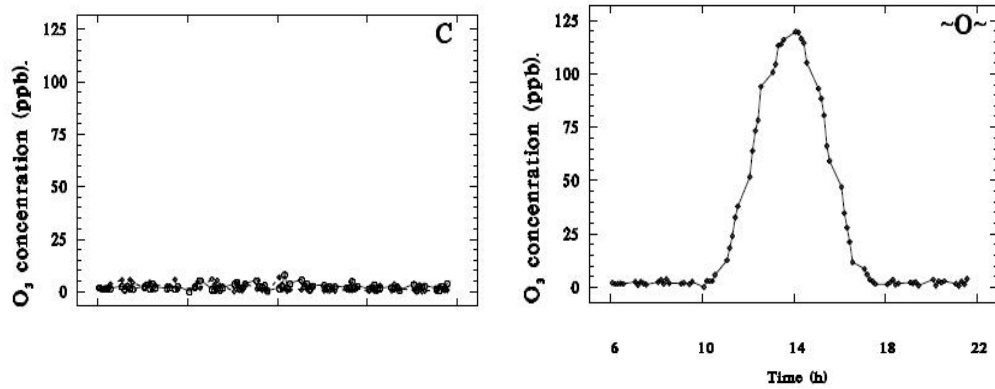


**Fig. 2.** The exposure regime for the O<sub>3</sub> (right) and ambient (left). The early O<sub>3</sub> was applied from 10:00 to 18:00h.

Illumination was supplied from a slide projector to the leaf through the slits in the cavity. Total white light intensity within the cavity was estimated to be  $530 \mu\text{mol m}^{-2}\text{s}^{-1}$  (PAR), obtained by halving the measured intensity at the surface of the cavity as per manufacturers's specifications. For far red light, obtained by using an optical bandpass filter (PTR Optics Ltd.), with 85% transmission at 710nm, the total intensity was estimated to be  $10 \mu\text{mol m}^{-2}\text{s}^{-1}$ . The cavity was at room temperature ( $24 \pm 3\text{C}$ ).

### ***Electron paramagnetic resonance (EPR)***

EPR spectra were obtained using a Varian E-line X-band spectrometer (Varian). A model 5256A frequency converter (8-18GHz) (Hewlett. Packard) was used to measure frequency and a gaussmeter (Varian) to measure magnetic field strength. An E102 microwave bridge (Varian) generated microwaves. The microwave generator was connected to an E238 TM110 cavity (EPR cavity) via a 3 cm wide waveguide. An overview of the cavity and insert is shown in Figure 3.

The arrangement for positioning the end of an attached leaf within the quartz insert was described by (Victor and Manivalde, 1992) and involved the loose attachment of the leaf to a T-shaped, cellulose acetate holder by means of cellulose adhesive tape with the lower leaf surface against the holder and the upper surface facing the cavity slits as shown in Fig. 3. At each hour the following EPR signals were recorded: first the signal in white light, then the signal in 710nm light and lastly the signal in darkness. Between each spectrum a 2 min period was allowed for adaptation. Each spectral measurement took 4min. Spectra were recorded between 11:00 and 16:00h. The leaves were maintained in white light between measurements. For spectral recording the EPR conditions employed were:

Sweep width:	250G,
Scan time:	4min,
Time Constant:	0.128s,
Power:	10mW
Detector current:	100 $\mu$ A,
Gain:	$5 \times 10^{-4}$

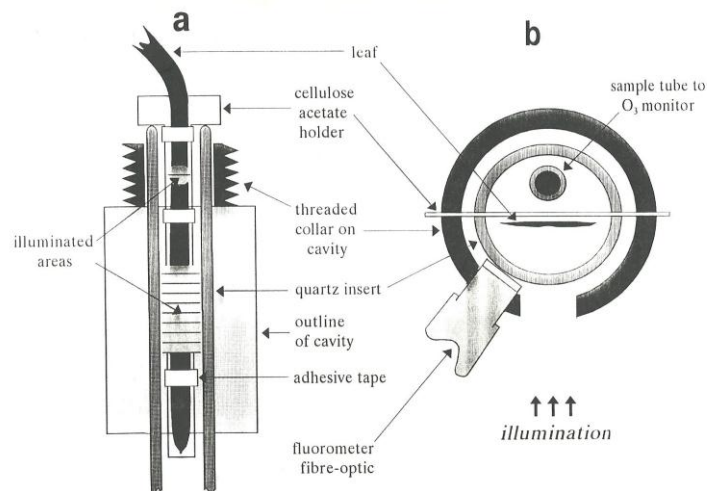


**Fig. 3.** Longitudinal (a) and cross-sectional (b) views of the cavity, showing the arrangement of leaf and leaf holder, the ozone sampling tube, the fluorometer fibre optic, and the illuminated areas of the leaf.

### ***Experimental design, spectra data handling, normalization and statistical analyses***

In each experiment, the two treatments were, control and O<sub>3</sub> treatment and n = 4 for treatment. Typical first-derivative EPR spectra are shown in Figure 4, illustrating the measurement of signal heights and showing *g*-values. In order to remove leaf-to-leaf variability the EPR signal height data were normalized to the value at 1100h (i.e. 1h after the start of the O<sub>3</sub> exposure wave). Additional experiments were conducted to examine the kinetics of Signal I changes resulting from changing light conditions. In these experiments, the leaves were mounted in the cavity at 10:00h and maintained in white light until the traces were recorded at 14:00h. Since the O<sub>3</sub> exposure wave started at 10:00h these traces were recorded at the time of the peak. Traces like the one shown in Figure 5 were collected with the system locked onto the low-field maximum of Signal I and the leaf in darkness or illuminated with 710nm or white light in various sequences. Since the low field maximum of the first derivative of Signal I occurs at approximately the same field strength as that at which the first derivative of Signal II is close to zero, i.e. the maximum of the Signal II absorption spectrum, the effect of any changes in signal II on the amplitude of the first derivative of Signal I is minimal (Blumenfeld *et al.*, 1974).

SYSTAT/SYGRAPH (Systat Inc.) was used for all statistical analyses and graphics. The DWLS (distance weighted least squares) function of

SYGRAPH was used for curve-fitting to depict EPR and fluorescence data. Unless otherwise stated the trends depicted were established by polynomial contrasts.

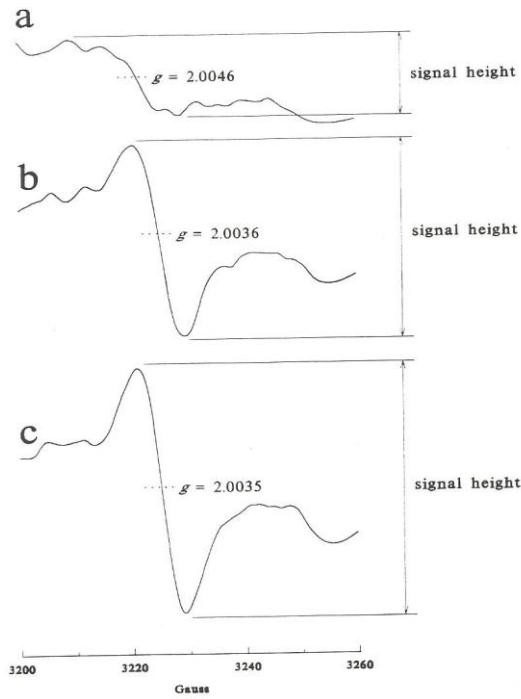


**Fig. 4.** Typical first derivative signals in a bluegrass leaf in a. Darkness; b. White light; c, 710nm light, illustrating height measurements and g-values ( $\pm 0.0002$ ).

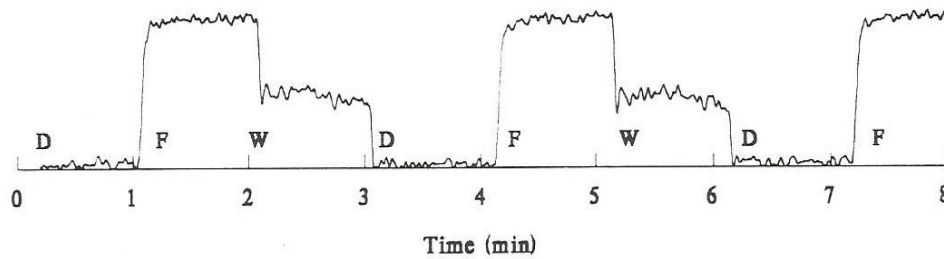


**Fig. 5.** Trace of Signal I low-field maximum in a bluegrass leaf in changing light conditions. D = darkness; F = 710 nm light; W = white light.

### ***Fluorescence measurements***

A Portable Fluorometer (Model PAM2000; H.Walz GmbH, Effeltrich, Germany) with integrated Poqet PQ-1024 computer was used to measure

fluorescence parameters. The parameters determined were derived from the measurement of  $F_0$ ,  $F_m$ ,  $F_m'$ ,  $F_t$ , defined as in Schreiber *et al.* (1978). The fluorescence parameters were measured on the first true leaf of one randomly selected plant from four pots for each treatment. Photochemical quenching (qP), non-photochemical quenching correlated with 'thylakoid membrane energization' (qN), non-photochemical quenching (reflecting heat dissipation of excitation energy in the antenna system) (NPQ), and fluorescence quantum yield (Y) were calculated as in Mazarura (2012b). As it was not possible to modify the cavity itself, the threaded section at the top of the cavity was adapted to accommodate the fibre optic cable of the fluorometer (Figures 1 and 3). A port for the illumination of the part of leaf viewed by the fibre-optic was provided to ensure that the same light intensity was used for both fluorescence and EPR measurements. These measurements were taken at the same time as EPR measurements at hourly intervals from 11:00 to 16:00h. In order to remove leaf-to-leaf variability the fluorescence parameters were normalized to the value at 11:00h, as described for EPR spectral data above.

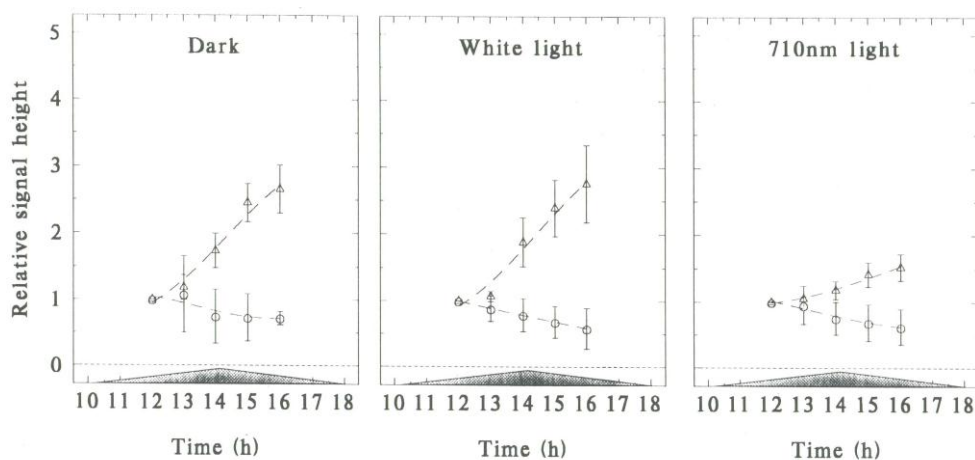


**Fig. 6.** Effects of  $O_3$  on relative signal height in the dark, white or 710nm light for Kentucky bluegrass. Control (O);  $O_3$  ( $\Delta$ ). Bars are SEDs based on individual means for each hour. N: 8.

## Results

### *Effects of $O_3$ on photosynthetic radicals*

Kinetic traces of the signals in darkness, white light and 710 nm light are given in Figure 6. The signal in white light (W) was larger than that in 710nm light (F) regardless of exposure to  $O_3$ . After exposure to W, switching to F resulted in a slow rise in Signal I in contrast to the rapid rise following D.

Ozone, however, caused a slight 2-phase lag in the saturation of the signal in W after D. Although Signal I in F rose faster after D than after W in the control, the low levels of Signal I in F make it impossible to determine whether similar differences in saturation rates occurred in the presence of  $O_3$ .

The white light signal (Signal I + II) increased slowly with time during  $O_3$  exposure (Figure 7) and it was significantly larger than the control after 15:00h. However, the signal in 710nm light showed more variability over time and although the signal in  $O_3$  was consistently higher than the control, the differences were only marginally significant (Figure 7). No dark Signal II could be reliably detected. In terms of absolute signal heights, those in white light were consistently greater than those in far-red light, regardless of exposure to  $O_3$ .

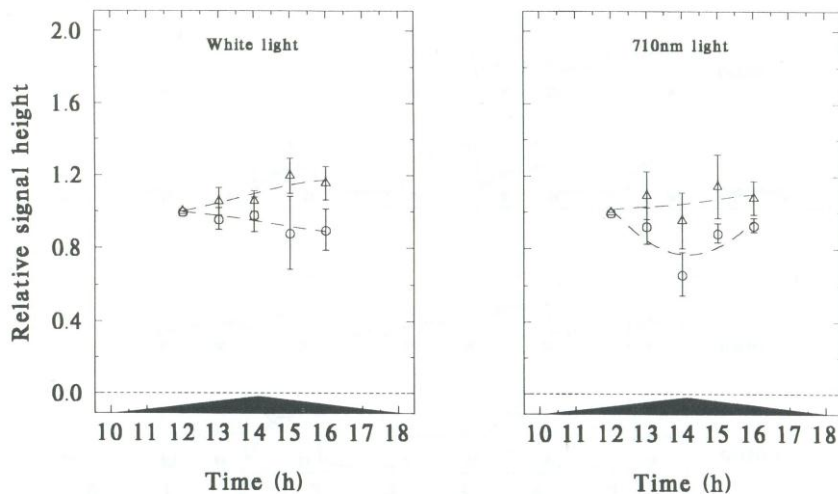


**Fig. 7.** Effects of  $O_3$  on relative signal height in the dark, white or 710nm light for Kentucky bluegrass. Control (O);  $O_3$  ( $\Delta$ ). Bars are SEDs based on individual means for each hour. N = 8.

### ***Effects of $O_3$ on chlorophyll fluorescence***

Ozone slightly stimulated relative quantum yield (Y) (Fig. 8a), and photochemical quenching (qP) (Fig. 8b). However,  $O_3$  increased both qN and NPQ significantly relative to the controls, which decreased over time (Fig. 8c and d, respectively).

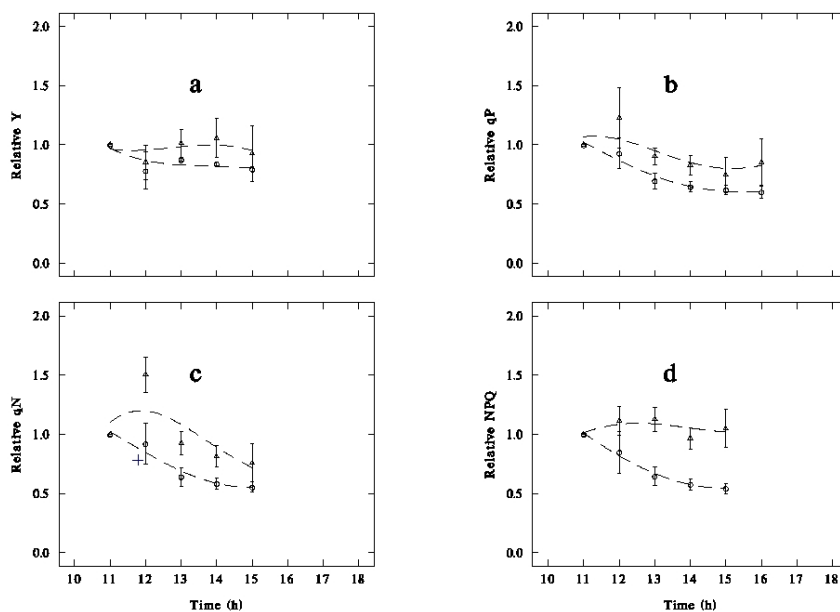


**Fig. 8.** Effects of O<sub>3</sub> on a. quantum yield (Y); b, photochemical quenching (qP); c, non-photochemical quenching (qN) and d, non-photochemical quenching (NPQ). (○) Control; (Δ) O<sub>3</sub>. Bars are SEDs, n=8.

## Discussion

The sluggish responses to different light exposures in foxtail suggest that the light intensities used were insufficient to cause rapid saturation of photosystem centers. However, the intensity of the far-red band used was only reduced about 15% relative to the 710nm component of the white light. Nevertheless, the greater signal I observed in white rather than 710nm in the foxtail leaf suggests greater light harvesting by PSI centers in white light.

Although it was originally thought that PSII was absent from the frequently granaless bundle sheath chloroplasts in C-4 plants, evidence from studies with *Zea mays* indicated that a form of PSII is present in the bundle sheath thylakoids, and that its light-harvesting complex (LHCII) functions as an antenna for the PSI present (Bassi *et al.*, 1995). Pfundel *et al.* 1996 showed that such involvement of light capture in the red region of the spectrum in the activation of PSI in bundle sheath chloroplasts also occurs in *Setaria viridis* and other C-4 species. This would account for the observations of greater Signal I levels in white than in far-red light in foxtail when in the C-3 grass, Kentucky bluegrass the signal in white was smaller than that in far-red light (Mazarura, 2012a).

The slow maximization of Signal I on switching from white to far-red light (Fig. 6) possibly results both from the low light intensity and the need for PSI centers to uncouple from LHCII and couple with LHCI antenna systems. Switching from 710nm to white light would require the reverse process, which seems to occur more rapidly as indicated by the faster increase to the maximum.

The dark signal II in foxtail was rarely distinguishable above the noise level but evident in Kentucky bluegrass, a C-3 grass (Mazarura, 2012a). This is surprising in view of the fact that between the hourly observations, the leaves were maintained in white light, and as a result would have been expected to demonstrate the slow Signal II component associated with the tyrosine residue (Y<sub>D</sub>) on the D2 protein.

During exposure to O<sub>3</sub> non-photochemical quenching (qN) decreased over time but remained higher than in the control (Fig. 8) while NPQ remained unchanged over time but also was consistently higher than in the control. This is in agreement with the fluorescence response observed in the presence of DCMU (Krause and Weis 1991) or atrazine (Bolhar-Nordenkampf *et al.*, 1989). These together with the O<sub>3</sub>-induced increases in non-photochemical quenching and the changes in EPR signals are compatible with the earlier suggestion that interference with water-splitting is a major consequence of exposure to O<sub>3</sub> (Shimazaki, 1988; Schreiber *et al.*, 1978).

Exposure to O<sub>3</sub> also resulted in increases in the EPR signals in white and 710nm light, (Fig. 7). The saturation of Signal I in white light was slower in O<sub>3</sub> than in the control (Fig. 6) again suggesting that O<sub>3</sub> was interfering with electron-flow to photosystem I. The minor increases in Signal I induced by O<sub>3</sub> were insufficient to lead to any significant changes in fluorescence yield or photochemical quenching. However, the increased non-photochemical quenching caused by O<sub>3</sub> may have been caused by effects on the water-splitting side of PSII.

In summary, the effects of O<sub>3</sub> revealed by the observed changes in Signals I and II are indicative of reduced electron flow through PSI, and through PSII. This suggests that the main effect of O<sub>3</sub> is on the electron acceptor side of PSII, and may involve impairment of the water-splitting process (Schreiber *et al.*, 1978). The observed O<sub>3</sub>-induced increase in both non-photochemical quenching parameters (qN and NPQ) are compatible with such an interpretation.

## References

- Barry, B.A. and Babcock, G.T. (1987). Tyrosine radicals are involved in the photosynthetic oxygen-evolving system. *Proceedings of the National Academy of Sciences* 84(20):7099–7103.
- Bassi, R., Marquardt, J. and Lavergne, J. (1995). Biochemical and functional properties of photosystem II in agranal membranes from maize mesophyll and bundle-sheath chloroplasts. *Eur. J. Biochem.* 233:709–719.
- Beinert, H., Kok, B. and Hoch, G. (1962). The light induced electron paramagnetic resonance signal of photocatalyst P700. *Biochemical and Biophysical Research Communications* 7(3):209–212.
- Blumenfeld, L.A., Goldfield, M.G., Tzapin, A.I. and Hangulov, S.V. (1974). Electron spin resonance signal I in leaves of higher plants: behaviour under simultaneous and separate illumination with red and far red light. *Photosynthetica* 8(3):168-175.
- Bolhar-Nordenkamp, H.R. et al., 1989. Chlorophyll Fluorescence as a Probe of the Photosynthetic Competence of Leaves in the Field: A Review of Current Instrumentation. *Functional Ecology*, 3(4), p.497.
- Bussotti, F., Desotgiu, R., Cascio, C., Pollastrini, M., Gravano, E., Gerosa, G., Marzuoli, R., Nali, C., Lorenzini, G., Salvatori, E., Manes, F., Schaub, M. and Strasser, R.J. (2011). Ozone stress in woody plants assessed with chlorophyll a fluorescence. A critical reassessment of existing data. *Environmental and Experimental Botany* 73:19–30.
- Calatayud, A., Iglesias, D.J., Talon, M. and Barreno, E. (2004). Response of spinach leaves (*Spinacia oleracea* L.) to ozone measured by gas exchange, chlorophyll a fluorescence, antioxidant systems, and lipid peroxidation. *Photosynthetica* 42(1):23–29.
- Calatayud, A., Iglesias, D.J., Talon, M. and Barreno, E. (2006). Effects of long-term ozone exposure on citrus: Chlorophyll a fluorescence and gas exchange. *Photosynthetica* 44 (4):548-554.
- Calatayud Angeles and Barreno Eva (2004). Response to ozone in two lettuce varieties on chlorophyll a fluorescence, photosynthetic pigments and lipid peroxidation. *Plant physiology and biochemistry: PPB / Société française de physiologie végétale* 42(6):549–555.
- Declaire, M., de Cat W., de Temmerman, L. and Baeten, H. (1984). Changes of peroxidase, catalase, and superoxide dismutase activities in ozone-fumigated spinach leaves. *J. Plant Physiol.* 116:147-152.
- Ding, Y.F. (2010). The role of miR398 in plant stress responses. *Hereditas (Beijing)* 32(2):129–134.
- Dizengremel, P. (2009). Metabolic-dependent changes in plant cell redox power after ozone exposure. *Plant Biology* 11:35–42.
- Heath, R.L. (1988). Biochemical mechanisms of pollutant stress. In W. W. Hecker, O. C. Taylor, & D.T. Tingey, eds. *Assessment of Crop Loss from Air Pollutants*. London: Elsevier Applied Science, pp. 259–286.
- Krause, G.H. and Weis, E. (1991). Chlorophyll Fluorescence and Photosynthesis: The Basics. *Annual Review of Plant Physiology and Plant Molecular Biology* 42(1):313–349.
- Lee, E.H. and Bennett, J.H. (1982). Superoxide dismutase. A possible protective enzyme against ozone injury in snap beans (*Phaseolus vulgaris* L.). *Plant Physiol.* 69:1444–1449.
- Mazarura, U. (2012a). Concurrent EPR and fluorescence studies of the effect of sequences of fluctuating low levels of ozone on Kentucky bluegrass. *Journal of Agricultural Technology* 8(7):1459–1474 (in press).
- Mazarura, U. (2012b). Effect of sequences of ozone and nitrogen dioxide on chlorophyll fluorescence in radish. *African Crop Science Journal* 20(2):473-485.

- Mudd, J.B. (1982). Effects of oxidants on metabolic function. In M. H. Unsworth & D. P. Ormrod, eds. *Effects of Gaseous Air Pollution on Agriculture and Horticulture*. London: Butterworth Scientific, pp. 189–203.
- Pfundel, E., Nagel, E. and Meister, A. (1996). Analyzing the Light Energy Distribution in the Photosynthetic Apparatus of C4 Plants Using Highly Purified Mesophyll and Bundle-Sheath Thylakoids. *Plant physiology* 112(3):1055–1070.
- Runeckles, V.C. and Vaartnou, M. (1997). EPR evidence for superoxide anion formation in leaves during exposure to low levels of ozone. *Plant, Cell & Environment* 20(3):306–314.
- Runeckles, Victor C. and Vaartnou, Manivalde (1992). Observations on the in situ detection of free radicals in leaves using electron paramagnetic resonance spectrometry. *Canadian Journal of Botany* 70(1):192-199.
- Schreiber, U., Vidaver, W., Runeckles, V.C. and Rosen, P. (1978). Chlorophyll fluorescence assay for ozone injury in intact plants. *Plant Physiol.* 61:80-84.
- Shimazaki, K. (1988). Thylakoid membrane reactions to air pollutants. In S. Schulte-Hostede et al., eds. *Air Pollution and Plant Metabolism*. London: Elsevier, pp. 116-133.
- Sunkar, R., Kapoor, A. and Zhu, J.K. (2006). Posttranscriptional Induction of Two Cu/Zn Superoxide Dismutase Genes in Arabidopsis Is Mediated by Downregulation of miR398 and Important for Oxidative Stress Tolerance. *The Plant Cell Online* 18(8):2051-2065.
- Wang, L., He, X. and Chen, W. (2008). Effects of Elevated Ozone on Photosynthetic CO<sub>2</sub> Exchange and Chlorophyll a Fluorescence in Leaves of *Quercus mongolica* Grown in Urban Area. *Bulletin of Environmental Contamination and Toxicology* 82(4):478-481.
- Zheng, Y. (2010). Effects of long-term ozone exposure on chlorophyll a fluorescence and gas exchange of winter-wheat leaves. *Huan jing ke xue= Huanjing kexue / [bian ji, Zhongguo ke xue yuan huan jing ke xue wei yuan hui 'Huan jing ke xue' bian ji wei yuan hui.]*, 31(2):472–479.
- Zhu, C., Ding, Y. and Liu, Haili (2011). MiR398 and plant stress responses. *Physiologia Plantarum* 143(1):1–9.

(Received 10 September 2012; accepted 30 November 2012)